NASA SP-5972 (04)

January 1975

TECHNOLOGY UTILIZATION

ANALYTICAL TECHNIQUES

A COMPILATION

NATIONAL AERONAUTICS AND SPACE ADMINISTRATION

Foreword

The National Aeronautics and Space Administration has established a Technology Utilization Program for the dissemination of information on technological developments which have potential utility outside the aerospace community. By encouraging multiple application of the results of its research and development, NASA earns for the public an increased return on the investment in aerospace research and development programs.

This document is one in a series intended to furnish such technological information. Divided into three sections, this Compilation contains articles on a number of analytical techniques that should be of interest to quality-control engineers and laboratory workers. Section 1 describes a number of techniques for testing electronic, mechanical, and optical systems. Section 2 contains a number of nondestructive testing techniques, and Section 3 presents several techniques for the analysis of gases.

Additional technical information on the articles in this Compilation can be requested by circling the appropriate number on the Reader Service Card included in this Compilation.

The latest patent information available at the final preparation of this Compilation is presented on the page following the last article in the text. For those innovations on which NASA has decided not to apply for a patent, a Patent Statement is not included. Potential users of items described herein should consult the cognizant organization for updated patent information at that time.

We appreciate comment by readers and welcome hearing about the relevance and utility of the information in this Compilation.

Jeffrey T. Hamilton, *Director*
Technology Utilization Office
National Aeronautics and Space Administration

Contents

SECTION 3. ANALYSIS OF GASES AND GAS-SUSPENSIONS

Section 1. System Test and Analysis

METHOD FOR OBTAINING ABSOLUTE LEVELS OF TAPE RECORDER FLUTTER

Flutter-Measurement Instrumentation

The flutter-measuring instrumentation shown in the figure can be used to determine the absolute amplitude values of tape recorder flutter. The technique consists of calibrating the percent peak deviation of flutter and then comparing this with the flutter on a constant-amplitude tone. Since commercial flutter meters are capable of indicating only the RMS level of flutter, the advantages of the new technique may justify the costly equipment involved.

The possible benefits that may accrue from the use of the system are the establishment of: (a) a method for correcting errors in data, due to tape recorder limitations, in the flow-frequency portion of the spectrum; (b) a procedure for comparing tape recorder capabilities; and (c) useful data to be used for designing equipment that must work with signals from a tape recorder. (Such equipment includes the phase-lock loop units that are often used to track tape-recorded signals.) The method may be useful to those interested in tape-recorded low-frequency data, tape recorder manufacturers and designers, instrumentation and signal-conditioning equipment designers, and telemetry system designers.

Circle 1 on Reader Service Card.

1

MEASUREMENT OF X-RAY SCATTERING BY OPTICAL SURFACES

The telescope, an instrument in existence for several centuries, is no longer only a visible light device. Indeed, different telescopes are being built for radio frequencies as well as for X-rays. Of the three basic designs, X-ray telescopes are the most demanding in precision. Optical surfaces built for X-ray telescopes are made to reflect very short wavelengths that range in magnitude from 2 to 100 angstroms. Minor irregularities or contamination on the surface of any telescope mirror can seriously affect the quality of an optical image at those wavelengths.

An apparatus has been developed for checking the reflection of optical surfaces intended for the 2- to 100-angstrom soft X-ray region. Scattering of X-rays can now be measured with angular accuracy of one arc-second.

The apparatus uses a vacuum system consisting of three stainless-steel chambers each 24 inches (61 cm) in diameter and 12 inches (30.5 cm) high. One chamber contains an X-ray detector, the second an optical sample, and the third an X-ray source. The three chambers are interconnected by a 6-inch (15-cm), internal diameter, stainless-steel tubing which runs perpendicular to the chamber axes. The center-to-center distance between the chambers is 17.2 feet (5.25 m). The two end chambers have their own pumping systems which produce a vacuum of 5×10^{-6} torr.

The arrangement as shown in the figure uses a demountable X-ray source consisting of a filament enclosed by a focusing cup mounted on insulators above an anode (details not shown). The X-ray source is continuously pumped and has exchangeable anodes, one of aluminum for 8.34-angstrom emission and the other of carbon for 44-angstrom emission. Accelerating voltage for the aluminum anode is 3.5 kV at 20 mA, while for the carbon anode it is 1.4 kV at 30 mA. The angle between the direction of the X-ray beam and the anode is 15°. A slit 0.002 inch (0.05 mm) wide is mounted directly in front of the anode to define accurately the beam width of the source.

The sample to be tested is mounted vertically in a holder which can be rotated in the horizontal plane in one arc-minute increments. A knife-edge spacing of 0.001 inch (0.03 mm) is provided by placing shims between the knife edge and the source.

Adjacent to the sample is a secondary detector which is used to monitor the direct beam from the X-ray source. Thus, any variation in beam intensity can be normalized by evaluating the ratio of counts in the primary and secondary detectors.

The primary detector located in the end chamber is mounted on a screw so that it can be translated across the scattered X-ray beam in 0.1 arc-second intervals. The detector is a flow-type proportional counter with a replaceable window. The window uses either the 1/4-mil (0.006-mm) aluminum for the 8.34-angstrom test or a 2-micrometer-thick Makrofol supported by a nickel mesh for the 44-angstrom test. A 0.002-inch (0.05-mm) slit is mounted directly in front of the detector window.

In use, the apparatus is aligned by means of a laser so that the angle of incidence between the sample and the source is proper. After alignment, the chambers are

closed and evacuated. The X-ray source is then turned on, and the reflected beam is recorded with the detectors. Inspection of the reflected X-ray beam will then reveal the effects of imperfections on the optical surface of the sample.

Source: R. S. Wriston of
Martin Marietta Corp.
under contract to
Goddard Space Flight Center
(GSC-11590)

Circle 2 on Reader Service Card.

DIRECT MODELING, PARAMETER SIGNATURE ANALYSIS, AND FAILURE-MODE PREDICTION OF PHYSICAL SYSTEMS USING HYBRID COMPUTER OPTIMIZATION

Hardware and techniques have been developed for the high-speed automated identification and system design of dynamic systems, both linear and nonlinear. The technique consists of inserting the proposed model in parallel with a function generator that provides an output identical to that of the actual system (in off-line identification) or identical to the desired output (in off-line system-synthesis problems).

An error signal is generated from the difference of the actual (or desired) output signal and the model output signal. A positive definite function of the error signal provides an index of performance P. The optimization program adjusts the model parameters until a minimum of the value of P is obtained. The output printer then provides the best parameters of the model and the best index of performance obtained. The response of the best model and the actual (or desired) response are available on an oscilloscope for high-speed systems or on a plotter for low-speed systems.

In addition, the facility for including general non-linearities in the system model has been added. This has resulted from the design and construction of a digital-controlled, nonlinear-function generator and the modification of the optimization program to control this device.

Applications include sound-velocity profile characterization and identification of nonlinear dynamic systems. Extensions now include the following: (a) the identification and design of multivariable linear dynamic systems, (b) the study of topological aspects of modeling nonlinear dynamic systems, (c) the development of models for the human operator as a system component, and (d) general-pattern classification.

The results of the hardware and the techniques developed include the following:

a. The failure-mode prediction has been implemented, tested, and verified in the laboratory;

b. The advantages of parameter signature analysis over signal signature analysis have been demonstrated in determining the present readiness of an existing system;

c. The optimization programs in use have been improved by including the Fletcher-Reeves algorithm, successive line searches, and the steepest descent starts in the hybrid computer mode of operation;

d. Modeling techniques have been applied to a physical example, and excellent results have been obtained in the identification of the position servomechanism, with no apparent noise problem; and

e. A digitally-controlled, nonlinear-function generator has been designed, implemented, debugged, applied, and documented. The cost advantage over now-available commercial models may be significant.

Source: R. L. Drake, P. F. Duvoisin,
A. Asthana, and T. W. Mather of
Tulane University
under contract to
Marshall Space Flight Center
(MFS-22604)

Circle 3 on Reader Service Card.

NEAR-RANGE ACOUSTIC-NOISE REJECTION USING A PAIR OF SENSORS
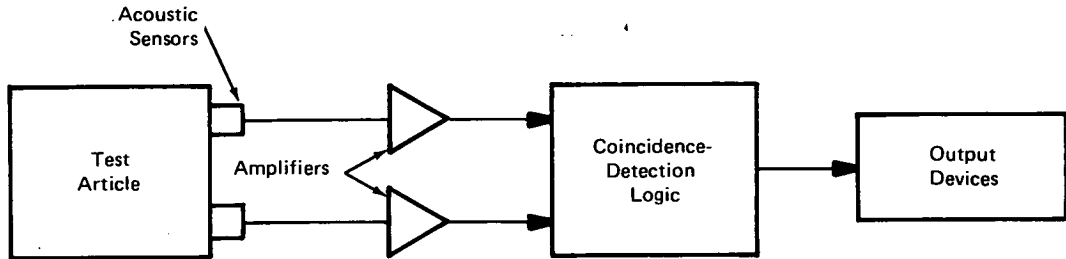
Block Diagram

The objective of the innovation shown in the figure is to eliminate acoustic noises occurring very close to a transducer. During the testing of composite structures, this noise elimination allows the acoustic-emission signals from subcritical crack growth to be detected as follows: In contrast to previous techniques, where mostly far-field noises were rejected, this system rejects numerous near-field noises. In addition, the circuit is insensitive to weak emission signals originating in the very close range of a sensor (where the signal strength changes most rapidly). Also the distribution of signal-detection sensitivity is more uniform than is possible with detection by a single sensor.

The coincidence-detection logic network compares the time relationship of the beginnings of two signals detected by the two sensors, and it produces a pulse output when the beginnings are coincident within a set time limit. This is performed by using a pair of level detectors of adjustable threshold, a pair of one-shot multivibrators of adjustable output-duration, and an AND gate. When the acoustic sensors are properly spaced, this detection logic rejects all noise signals originating at very close range to one sensor, because they are not detected by the other sensor. Several pairs of sensors may be combined to make a larger array of sensors, to cover a wider area than is possible with a single pair.

No further documentation is available.

VIBRATION PERFORMANCE NOMOGRAPHS FOR SUPPORTING STRUCTURES
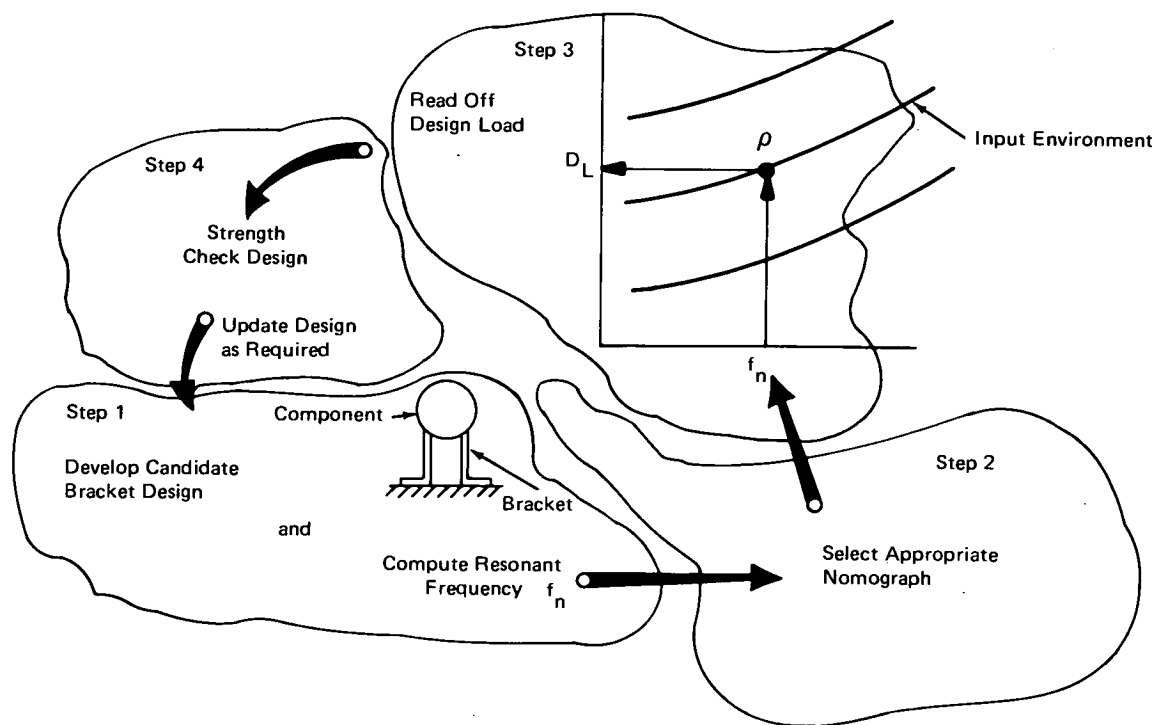
Nomograph Design Procedure

Statistical analyses are used to present the results of vibration tests on aluminum struts and other structural components as a series of design nomographs. Standard values of sinusoidal and random excitation are established as a function of resonant frequency. A suggested design procedure using these nomographs is shown in the figure. The nomographs are constructed with a 95-percent confidence level of excitation values, and they should expedite and aid in the design and development of bracket and other structural element configurations.

Dynamic magnification factors (Q) are calculated from the input and response vibration data for specific component and bracket parametric categories. These categories are statistically analyzed by linear regression, correlation, and regression variance analyses.

Source: F. A. Lehner of
The Boeing Co.
under contract to
Marshall Space Flight Center
(MFS-15236)

Circle 4 on Reader Service Card.

TECHNIQUE TO REDUCE DISTORTION IN ELECTRODYNAMIC VIBRATION SYSTEMS

Force

+

−

Normal Field Technique

Force

+

−

Reduced Field Technique

Force Signal at Resonance
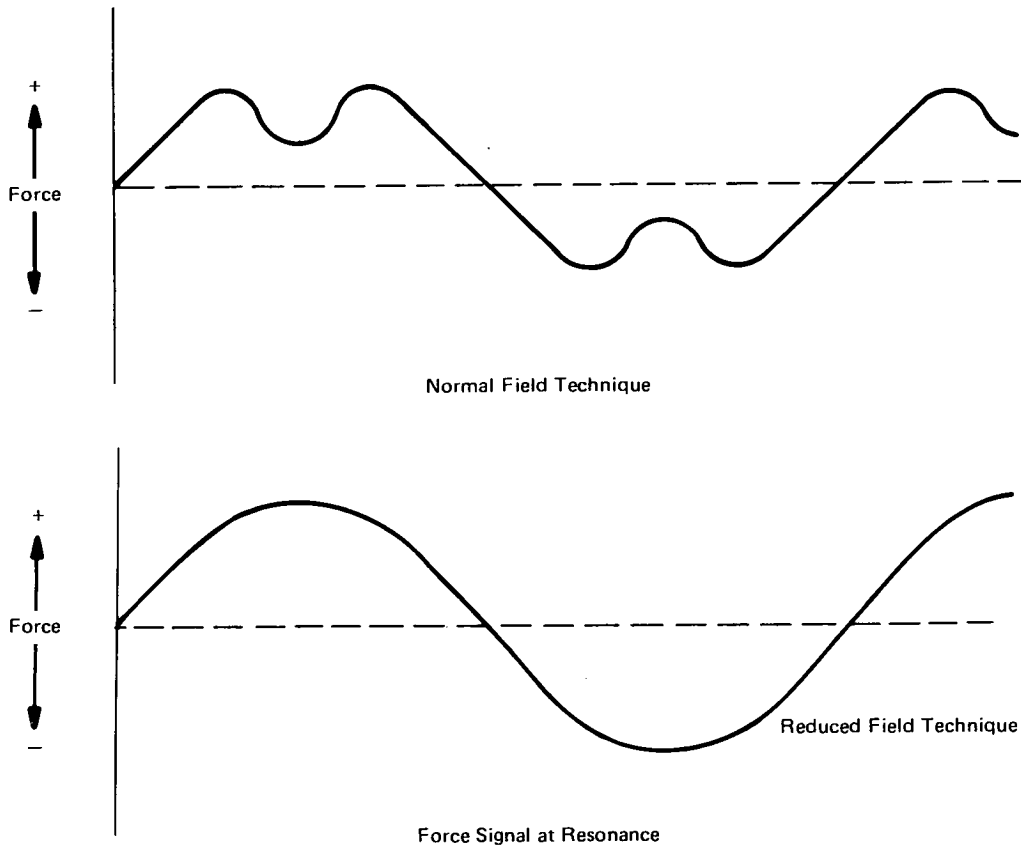
In a standard vibration testing system, a low-level sinusoidal signal is amplified and applied to a thruster armature that is connected to a structure under test. The resulting electromotive force between the armature current and a high-density magnetic field, created by dual field coils in the thruster, results in the desired motion and force level. The principle of this type of thruster is the same as that of an electrodynamic radio speaker.

With this system, excessive distortion of the applied force may make the data unusable for analysis. Such distortion originates in the reaction of the large structure. as it moves in the saturated electromagnetic field at resonant frequencies. A technique has been developed in which the electromagnetic field is reduced to obtain a distortion-free force level at such frequencies.

The force-level reduction is accomplished in several steps from 25 percent of the rated force level and one-third of the normal field current. The force signals arising from the normal field and the reduced-field technique are shown in the figure. Industries that might apply this technique include automative and aircraft manufacturers, railroads, shipbuilders, and other manufacturers of large heavy equipment and structures that require dynamic testing.

Circle 5 on Reader Service Card.

MULTISPECTRAL IMAGERY FOR DETERMINING
INFESTATIONS OF SOUTHERN PINE BEETLES

The southern pine beetle (*dendroctonus frontatis* Zimm) is the most destructive insect in the southern yellow pine (*Pinus spp.*) forests. The insect often reaches epidemic stages and is responsible for millions of dollars in damage each year. The biggest problem in combating the southern pine beetle is the detection of the infested trees. The most common method of detection is by aerial observers, who sketch the locations of the dead trees on a map. However, an observer may fail to detect all the infested trees and may make errors in plotting their locations.

A study has shown that, during the fall coloration period, multispectral photography and false-color images might be used to detect beetle-infested stands. Multispectral imaging involves the acquisition and comparison of two or more images of the same scene, recorded simultaneously in different parts of the electromagnetic spectrum (from the ultraviolet to the near-infrared). In the study, images are recorded on black-and-white infrared film (Kodak 2424) in four spectral bands of the following wavelengths:

1. Blue	400-480 nanometers
2. Green	480-590 nanometers
3. Red	590-700 nanometers
4. Infrared	730-900 nanometers

The camera used has lenses having 150-mm (6.0-in.) focal lengths, boresighted to view the same scene simultaneously. A focal plane shutter insures that each band receives fixed, repeatable exposure times. The square images are each 9.27 cm (3.65 in.) per side, on a standard aerial photograph format 22.9 cm (9 in.) square.

The photographs may be projected on a viewing screen individually or superimposed, and with or without filters. If the blue, green, and red bands are used with no filters, a black-and-white image will be produced, very similar to the one obtained on panchromatic film. If the infrared band is added, a black-and-white infrared image will result. Reconstructed color can be obtained by projecting each color band through a filter of that color.

False-color infrared images can be obtained by projecting the green band through a blue filter, the red band through a green filter, and the infrared band through a red filter. By selecting the proper band and filter combinations, details may be enhanced, often providing information not readily available through ordinary aerial photography.

In particular, the infrared portion of the electromagnetic spectrum can be used to distinguish hardwoods from conifers. In black-and-white infrared, the conifers will appear as a darker shade of gray; in false-color infrared, the conifers will be dark red with the hardwoods generally lighter. Discolored pines will appear blue or gray in false-color infrared.

During the growing season, the trees killed by the southern pine beetle can be detected on normal color photographs which can be reconstructed from multispectral imagery. However, false-color infrared and false-color images can be used to accent the difference between the hardwoods and the pines. The best images seem to be created by projecting the red band through a red filter and the infrared band through a green filter. Then the pine stands appear as a uniform dark green color with dead pines appearing brown. The hardwoods appear in lighter green and in shades of reddish brown. By careful observation an interpreter can identify hardwood stands and eliminate them from consideration.

An investigation is being continued to determine if false-color images obtained from multispectral photography are superior to normal color photography for this purpose. Investigations using high-altitude photography will also be conducted to determine if it can be used to reduce the time required for surveying the area.

Circle 6 on Reader Service Card.

VIBRATION MEASUREMENT BY PULSE DIFFERENTIAL HOLOGRAPHIC INTERFEROMETRY

A pulsed differential holography technique has been devised to measure structural deformations of materials that are subjected to a wide range of temperatures and other environmental conditions.

Continuous wave, time-average laser holography has been established as a method for mapping the displacements of a vibrating structure at ambient temperatures. At elevated temperatures, however, this method is severely limited by distortions induced by convection currents in the atmosphere adjacent to the test structure.

The effects of convection currents are eliminated by operating a pulsed laser in a double pulse mode which exposes the hologram two times in quick succession. During the exposure separation, the structure will deflect, but the turbulence in the medium will not change sufficiently to appreciably alter the optical path of the laser light and its reflection.

While this technique requires additions to existing pulsed holography setups, double pulsing should prove to be useful for measuring flutter, aerolastic, and other vibration characteristics of metal plates, beams, shells, and other structures. It is now possible to accomplish large area holography and to measure vibrations with large amplitudes. It is also no longer necessary to isolate the test structure in a vacuum chamber in order to eliminate or reduce atmospheric interferences.

Pulse differential holography is a variation on double-exposure holography, in which an interferogram is recorded. In this technique, a hologram is made of the test object. The object is then subjected to loads which cause it to deform, and a second hologram is made on the same piece of photographic film. Two images are produced when the developed film is illuminated by a laser light, one image from the undeformed object and the other when it is deformed. The light waves which form the two images interact with each other to create interference patterns. Analysis of the patterns reveals the surface deformations of the object caused by the load.

The timing of the two exposures, in pulsed differential holography, is carefully controlled to be synchronized with the deflection of the object being measured. The optimum time interval between exposures is dependent on several factors such as the number of fringes desired, vibration amplitude and frequency, and temperature of the structure. Too long a period between pulses results in fringes that are perturbated by the convection currents surrounding the object, while the shorter time intervals permit operation at higher temperatures and higher vibration amplitudes or frequencies.

The magnitude of the structural deformation is determined by counting the number of interference fringes that appear on the hologram. The first dark fringe corresponds to a deflection of one-quarter wavelength of the laser light being used, the second corresponds to three-quarters of a wavelength, and so on. The larger the slope in the surface of the object, caused by bending or deflection from an impact or other vibration-producing mechanism, the closer the spacing between fringes.

Using this technique, vibration amplitudes have been successfully measured on stainless steel panels heated to temperatures from 394 K (250° F) to 1394 K (2050° F). For these experiments the pulse duration was 50 x 10^{-9} second, while the interval between pulses was 50 microseconds.

The following documentation may be obtained from:

National Technical Information Service
Springfield, Virginia 22151
Single document price $3.00
(or microfiche $2.25)

Reference: NASA CR-2028 (N72-29543), Pulsed Differential Holographic Measurements of Vibration Modes of High-Temperature Panels

Source: D. A. Evensen and R. Aprahamian of
TRW, Inc.
under contract to
Langley Research Center
(LAR-11092)

REAL TIME STATISTICAL ANALYSIS OF ACOUSTIC
EMISSION SIGNALS FOR FLAW-MONITORING SYSTEMS

Acoustical signals are a useful means for detection of flaws in physical structures. Small structures are checked this way by monitoring the samples for acoustical signal count or count rate. Any flaws in the structure are located by observing the relatively high acoustical activity within a given area of the sample. Large structures, however, are more difficult to analyze this way because of the greater areas that must be monitored.

Based on the technique used in small structures, acoustical monitoring has been extended to large structures by dividing the large samples into small areas and then by monitoring each individual area separately.

The sample used in this development is a 105-in. (263-cm) diameter tank which consists of 3480 areas each approximately 10 in.^{2} (63 cm^2). The tank surface is proportioned to allow the layout of 20 equilateral triangles in the form of a slightly distorted icosahedron. Twelve transducers are equally positioned on the tank surface at the vertex of each of these triangles. The equilateral triangles are slightly elongated to account for the small cylindrical section of the tank, but are otherwise identical in size and shape. The system is divided into two distinct data handling segments, an analog and a digital.

The first segment operates in the analog mode and continuously monitors input signals from each transducer. Approximate location of the acoustic event is obtained by processing signal detection sequences and delay. This data is packed in the binary form and passed to the digital computer for further processing.

The second segment operates in the digital mode. Delay information from the analog unit is processed to provide an exact location of the acoustic event. The surface of the tank is divided into 3480 areas. A digital computer contains separate storage locations corresponding to each of these areas. A running sum of all acoustic activity is maintained in these storage locations by the digital computer. System operation is controlled through a standard teletypewriter. The data received and stored in the computer can be requested by the operator at any time and in any form that he desires.

Although noise rejection is used throughout the system, i.e., dual element transducers and bandpass filters, a constant background or random noises uniformly raise the totals of a large number of signal counts from all the storage areas. In this technique, a growing flaw area is localized and easily identified using the statistical capabilities of the on-line computer. For example, mean averages can be obtained of desired specific sub-areas of the entire tank at any time. The rate of emission signals for any given time can also be obtained. Statistical calculations are obtained from all input data in less than one second.

Source: F. E. Sugg and F. J. Moskal of
Rockwell International Corp.
under contract to
Marshall Space Flight Center
(MFS-24402)

Circle 7 on Reader Service Card.

RADIATION WINDOW CONNECTING TWO THERMALLY ISOLATED ENCLOSURES

An analytical method has been developed to estimate the radiation interchange between two radiation enclosures connected by an idealized thermal transfer medium (radiation window). The results are then used to help in the design or modification of complex thermal networks. The method is based upon the construction of a scale model of the network under study, using two precisely configured and aligned enclosures separated by a thermal transfer medium (radiation window).

The radiation window radiates in both directions; energy which might pass directly from enclosure #1 to enclosure #2 is first absorbed by the window. Part of this energy is then emitted directly back into the enclosure from which it came. The technique may be useful to individuals and organizations engaged in the research and development of all-electric home heating and air-conditioning systems, as well as electric ranges and microwave ovens.

Source: R. V. Weatherford of
Rockwell International Corp.
under contract to
Johnson Space Center
(MSC-19251)

Circle 8 on Reader Service Card.

TECHNIQUES AND SYMBOLS FOR ASSURANCE REVIEWS OF COMPLEX SYSTEMS

The group of symbols and the simplified method of diagramming large and complex electrical, pneumatic, and hydraulic network systems, for analytical and topographic pattern-recognition purposes, also may be used to permit circuit and design integrity reviews. Potential circuit problems, including potential single-failure points, relay races, component overloads, undesired circuit interactions, incorrect timing, interface compatibility, and undesirable transient conditions, can be detected more easily with the schematic drawings.

An analytical method of reducing electrical-system schematic complexity by the selective reduction of detail also provides a new analytic tool: the topographic symbology, complex pneumatic and hydraulic networks can be analyzed with approximately the same effort as electrical networks.

Source: J. P. Stapleton of
General Electric Co.
under contract to
Marshall Space Flight Center
(MFS-22144)

Circle 9 on Reader Service Card.

Section 2. Nondestructive Testing

COMPUTER-CONTROLLED VIBRATION TESTING

Conventional closed-loop analog vibration testing systems cannot provide real-time displays of test specimen response during test, and their performance cannot be corrected during a test because time constants, filter bandwidths, and other control functions cannot be readily altered. Moreover, conventional systems cannot be fully automated for analog control of random noise testing, and they inherently are subject to drift and must be periodically recalibrated.

A digital control system which is completely under computer command has been constructed to make possible fully automated control of random-noise vibration tests. The system is capable of providing real-time analysis with a continuously improving confidence level, and because the computer-controlled system can be preprogramed, it is possible to verify spectral test patterns prior to actual testing and to avoid operator error in setting up test parameters.

Preprogramed test specifications can be either tape-fed or introduced by a conversational computer language. Test excitation is produced by pseudo-random noise generated by digital techniques, but the excitation, although seemingly random in nature, has a predictable format; accordingly, randomness is injected in a manner which introduces very little variance into the power spectral density (PSD). This feature makes it possible to estimate the output PSD to a given confidence level much more rapidly than is possible with the purely random excitation that is obtained from Gaussian noise generated by the usual analog techniques. Precisely reproducible test spectra can be generated at any time.

The digital control system includes a Fourier processor, which is a special-purpose computer with a hard-wired, built-in algorithm for effecting a fast Fourier transform of time samples of the acceleration signal. The Fourier processor is in communication with the minicomputer of the digital control system via a specially-designed interface, and the transforms are used to compute the relative amplitudes of the frequency components in the observed test spectrum.

Estimates of the PSD are produced in the minicomputer by averaging the square of the moduli of the successive transform outputs from the Fourier processor; the estimates are in terms of bandwidth, resolution, and confidence level. The average test spectrum thus obtained is compared with a reference spectrum to produce a resultant in the form of an amplitude spectrum. This is multiplied by the pseudo-random noise signal and the resultant is subsequently transformed by a novel double sum-and-difference technique to produce a digital signal which can be converted to analog form for driving the excitation system.

During the test, the spectral response is displayed on a cathode ray tube which is integral with the Fourier processor, and a digital plotter is interfaced with the computer to plot results upon completion of the test. Test results are expressed as a power spectrum and in spectral ratios.

Some of the attractive features of the vibration testing system are: the short time required to reach a steady state, the increased accuracy of spectrum definition (there are no gaps as in the conventional noise sources), and a true Gaussian amplitude distribution of the resulting signals.

The computer-controlled vibration testing system possibly can be used for controlled shock-tests; for example, with the described system, it is possible to introduce initially the response characteristics of the total test system, and then to devise an input pulse which can produce the desired acceleration transient. Such a test would be operated as a semi-closed loop system.

Circle 10 on Reader Service Card.

AN INEXPENSIVE AND EFFECTIVE METHOD FOR
CALCULATING THE STRENGTH OF RANDOMLY REINFORCED FIBER COMPOSITES
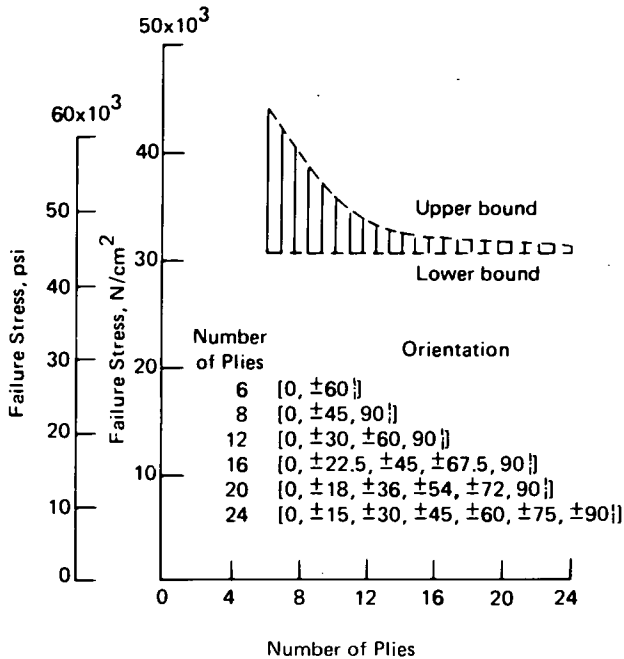
Upper and lower bounds for strength of various pseudoisotropic composites from Modmor-1/epoxy at 0.50 fiber volume content with zero voids and no residual stress.

Number of Plies	Orientation
6	$[0, \pm 60]$
8	$[0, \pm 45, 90]$
12	$[0, \pm 30, \pm 60, 90]$
16	$[0, \pm 22.5, \pm 45, \pm 67.5, 90]$
20	$[0, \pm 18, \pm 36, \pm 54, \pm 72, 90]$
24	$[0, \pm 15, \pm 30, \pm 45, \pm 60, \pm 75, \pm 90]$

Planar randomly reinforced fiber composites (PRRFC) can be made from any combination of a large number of available fibers and matrices. Selecting the most suitable combination for a given application usually leads to a time consuming and costly series of screening tests. An analytical procedure to determine the strength of PRRFC can serve as an effective and inexpensive means in selecting suitable fiber/matrix combinations for specific designs.

It has recently been demonstrated that the well-known laminate theory can be applied to determine the strength of PRRFC. A PRRFC is, in essence, a pseudo-isotropic laminate with a large number of ply orientation combinations where the strength is a function of these ply orientation combinations. The strength of the pseudoisotropic laminate, and thus the strength of PRRFC, can be predicted using laminate theory.

Laminate theory is used to demonstrate numerically that the minimum strength of a pseudoisotropic laminate is independent of the number of ply orientation combinations. The upper bound on the strength of a pseudo-isotropic laminate approaches the lower bound of its strength as the number of ply orientation combinations increases (see figure). Since a PRRFC is a pseudoisotropic laminate with a large number of ply orientation combinations and since the maximum strength of the pseudo-isotropic laminate approaches its minimum strength as the number of ply orientation combinations increases, it follows that the strength of the PRRFC is equal to the minimum strength of the pseudoisotropic laminate. This establishes the validity for using pseudoisotropic laminate analogy to predict the strength of PRRFC.

Laminate theory in conjunction with composite micro- and macromechanics can be used to predict mechanical properties of PRRFC's with any fiber/matrix combination. This procedure can also be used to investigate the effects of processing variables, such as cure temperature and void content, on the PRRFC strength. The pseudoisotropic laminate analogy applies to both fiber/metallic and fiber/nonmetallic matrix composites.

The simplest pseudoisotropic laminate which possesses bending symmetry suffices for strength predictions of PRRFC. One such laminate consists of the following ply orientation $(0°, +45°, -45°, 90°, 90°, -45°, +45°, 0°)$.

The following documentation may be obtained from:
National Technical Information Service
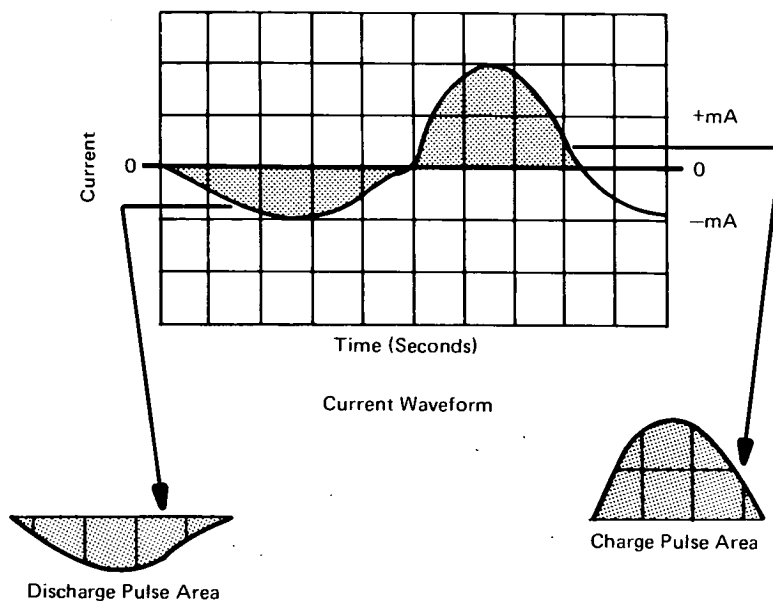Springfield, Virginia 22151
Single document price $3.00
(or microfiche $2.25)
Reference: NASA TN-D-6696 (N72-18582), Design Properties of Randomly Reinforced Fiber Composites

Source: Christos C. Chamis
Lewis Research Center
(LEW-11985)

QUICK METHOD FOR MEASURING WAVEFORM AREA IN PHOTOGRAPHS

Measuring Waveform Area

A fast and accurate method for measuring waveform area involves simply weighing portions of the photograph. The technique is substantially faster than using a planimeter when measuring the area of a plane figure of complex shape.

As an example, a pulsating current waveform is shown in the figure on a background of centimeter squares. The abscissa is time in seconds and the ordinate is current in milliamperes. The area under the waveform has dimensions of milliampere-seconds. The area enclosed by the waveform and the axes may be approximated by (a) taking a picture of the waveform on the oscilloscope screen, (b) carefully cutting out the resulting figure along the axes and the wave, and (c) weighing the cuttings. This weight then is divided by the weight of the photographic image of a single square, as determined by cutting out and weighing a block of such squares and dividing this weight by the number of squares in the block. This measurement technique could also be helpful in a vibration laboratory.

No further documentation is available.

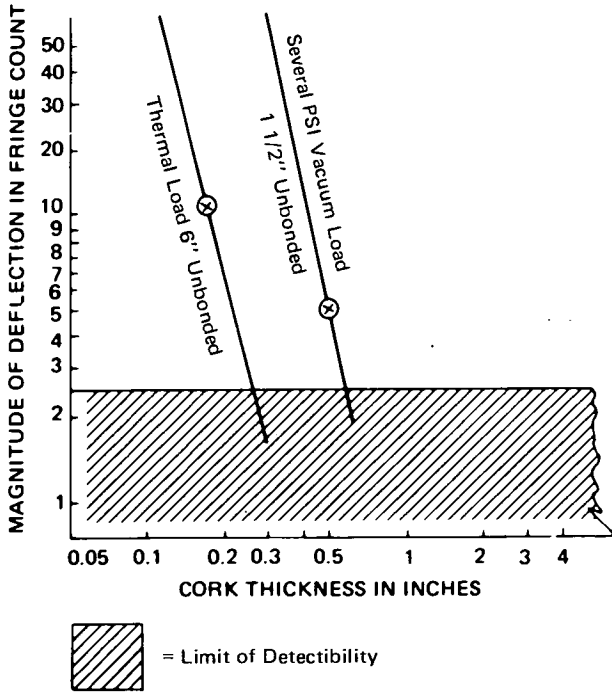# HOLOGRAPHIC NONDESTRUCTIVE TESTING OF LAMINATES

Figure 1. Log-Log Plot of Defect Indication and Cork Thickness
for Holographic Nondestructive Testing of Bonded Cork

Holography, a form of laser beam photography, is a relatively new technique that is being increasingly used for quality control testing. For instance, laminated structures in which two pieces of like or unlike materials are bonded together by an adhesive can be checked for bond quality through holography. Even with a common laminate such as plywood it is difficult to discover the existence of unglued portions without tearing the structure apart. With laser beam photography, however, very small differences in the laminate thickness result in interference fringes in the holograph image. These indicate the presence of an unbonded area.

There has in the past been a major drawback to this technique. For each laminate tested, the method had to be "calibrated" by checking a large number of known defective laminates. A new method circumvents much of the needed pretesting by considering the unbonded area to be a sort of membrane. In this way, theoretical knowledge of membrane deflection may be used in conjunction with a much reduced number of pretest experiments to determine the number of optical fringes that should appear for a given laminate. This information can then be directly related to the characteristics of unbonded areas.

The method consists of fitting experimental data to the equation.

$$\log \Delta l = 4 \log d - 3 \log t + \log q = K \qquad (1)$$

where Δ is fringe displacement,
         d is the diameter of the unbonded area,
         t is the facing sheet thickness,
         q is the loading factor, and
         K is a constant.

It is first necessary to establish a relationship between deflection and laminate thickness for different sizes of unbonded areas and various types of loading. A simplified form of equation (1),

$$\log \Delta = -3 \log t + K' \qquad (2)$$

where K' is the intercept constant,
is used with test points to develop data for the system. Figure 1 was plotted from equation (2) and test points. It shows the observed deflection versus laminate thickness for a bonded cork system. In this experiment the holographic test equipment permitted resolution of the fringe count to 2 1/2 fringes. From the results of Figure 1, a graph as shown in Figure 2 can be used to find the minimal detectable bond-void in terms of laminate thickness. The lines are based on the following relationship.

$$\log \Delta l = -3 \log t + 4 \log d + k = \text{a constant} \qquad (3)$$

or $\log d = 3/4 \log t + k'$

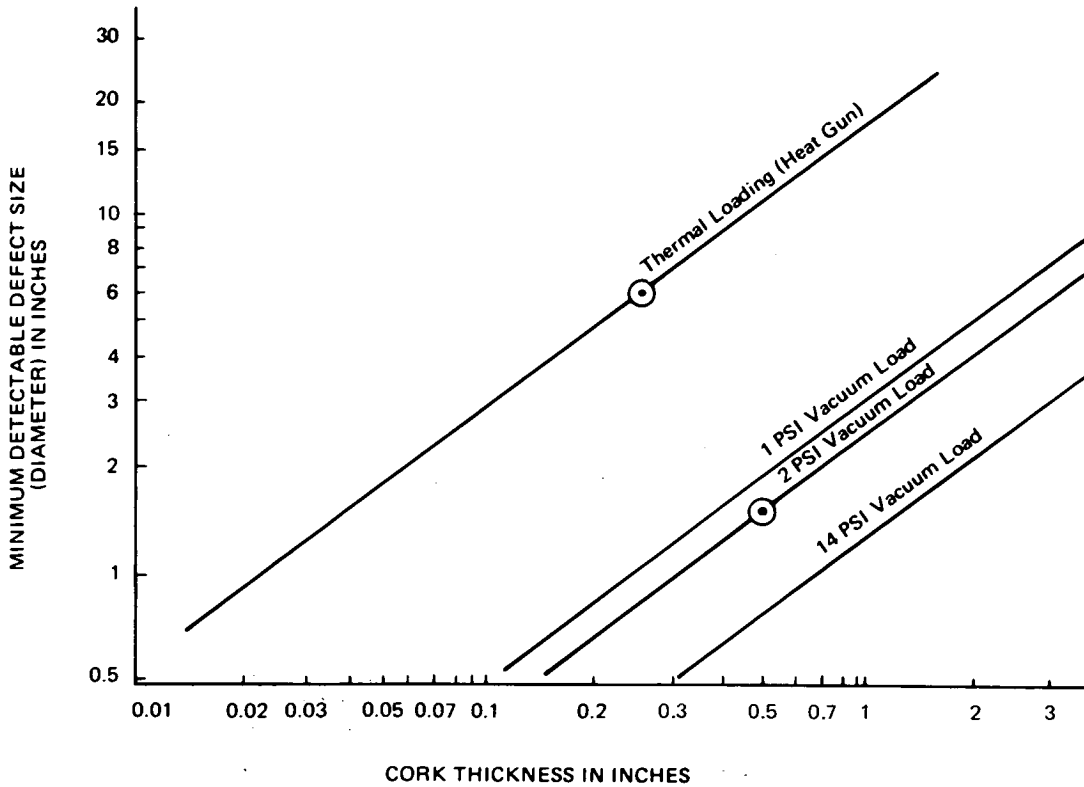where k and k' are intercept constants.

Figure 2. Log-Log Plot of Minimum Detectable Void Size versus
Cork Thickness Based on Theory and Experimental Size

To show the effect of increased vacuum loading, another term must be included in equation (2) to give

$$\log d = 3/4 \log t - 1/4 \log q + K''$$

where q is the vacuum loading in psi and K'' is the intercept value.

In Figure 2, experimental values of d, t, and q were used to find the value of K''. The calculated K' was then used to find the curves for 1 and 14 psi.

This method can be applied to any adhesive bonded facing that has membrane characteristics over unbonded areas. It allows prediction of the applicability of holographic testing with a minimum of experimental effort.

Source: F. H. Stuckenberg of
Rockwell International Corp.
under contract to
Johnson Space Center
(MSC-19107)

No further documentation is available.
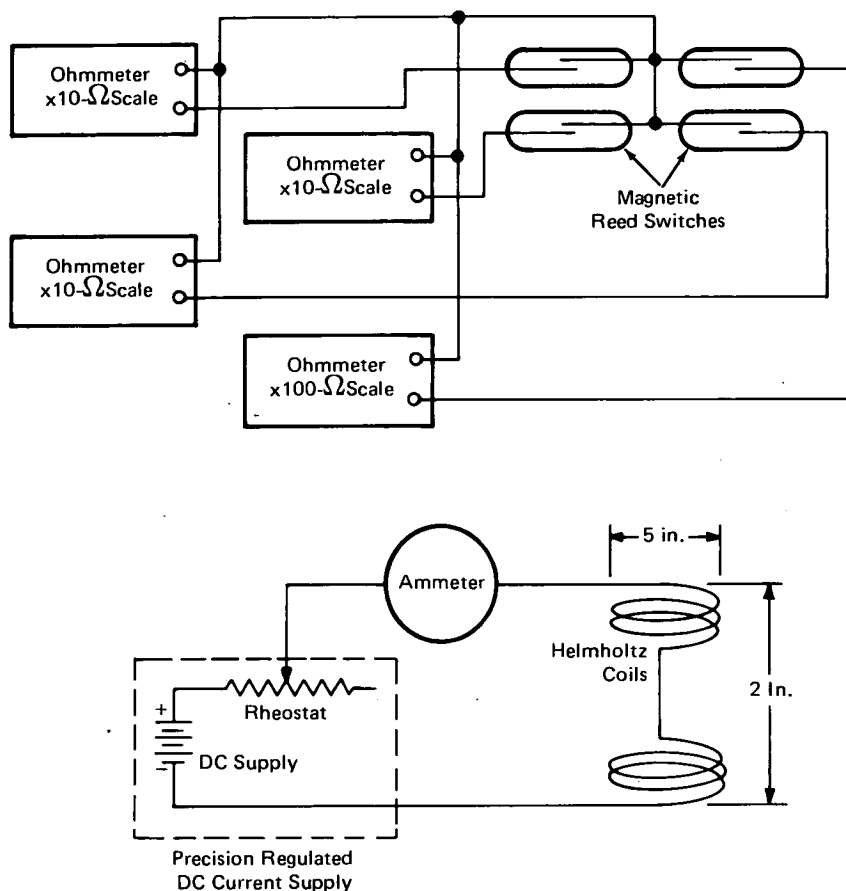
REED SWITCH TEST AT CRYOGENIC TEMPERATURES: A REPORT

Figure 1. Test Setup Schematic

A new report gives information on the performance of selected reed switches at temperatures below 89 K (−300° F). Previous work has provided data for temperatures above this range. Reed switch samples from two different manufacturers were subjected to temperatures approaching that of liquid helium, 19.3 K (−425° F).

There were two main test objectives. The first was to verify that the reed contacts would make and break. The second objective was to obtain data on the variation in current for pull-in and dropout as a function of temperature. Due to the extremely low temperatures involved, it became necessary to limit the heat losses to an absolute minimum; therefore the lead wires to the switches were made of number 38 Manganin wire which has a resistance of about

80 ohms. The maximum current and voltage which could be applied to the switches were 21.5 mA at 3.0 V. A schematic of the test setup is shown in Figure 1.

The test was performed by evacuating a chamber containing the test specimens and backfilling this chamber with helium to a pressure of 18.66 N/m² (140 μm of Hg). The outer chamber was then filled with liquid nitrogen until temperature stabilization had been reached, at which point liquid helium was introduced into the inner chamber (Figure 2). As the temperature decreased toward 89 K (−300° F) all four switches were actuated periodically. The coil current for pull-in and dropout of each switch was recorded as a function of temperature. After the switch had stabilized with liquid nitrogen in the outer chamber and liquid helium had been
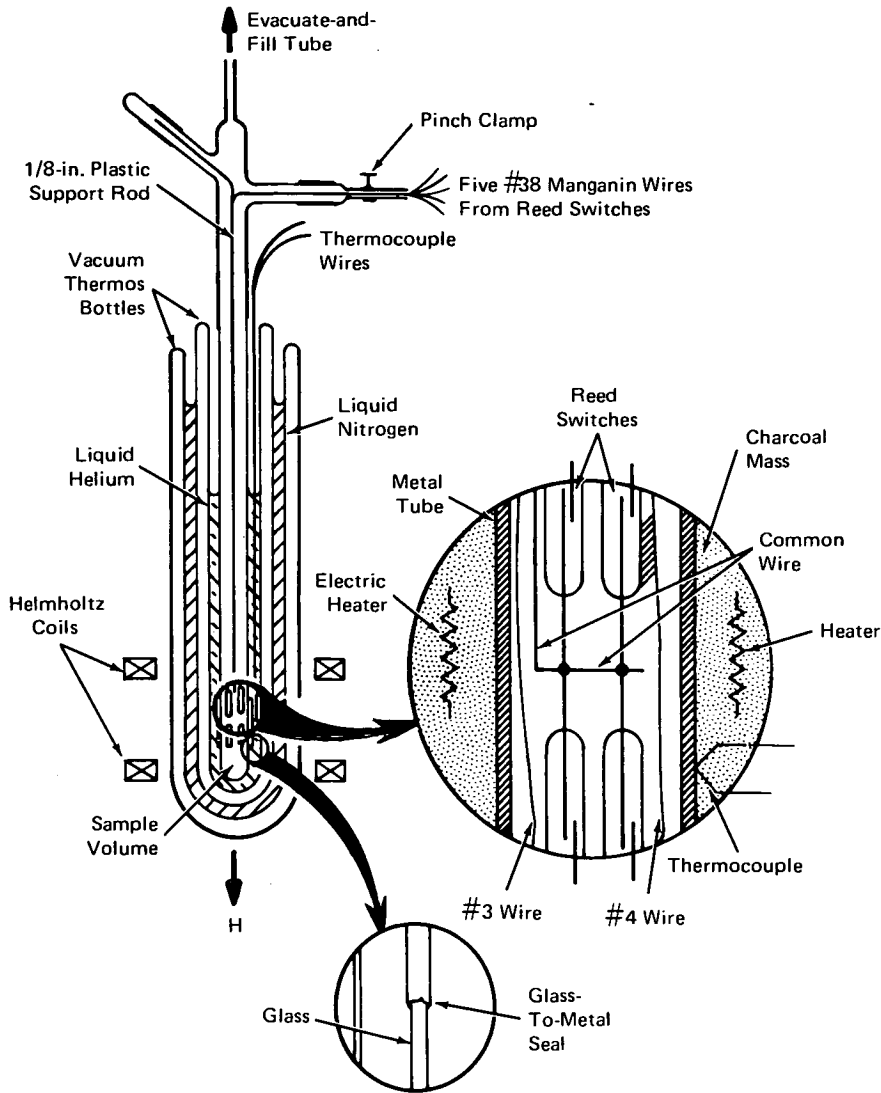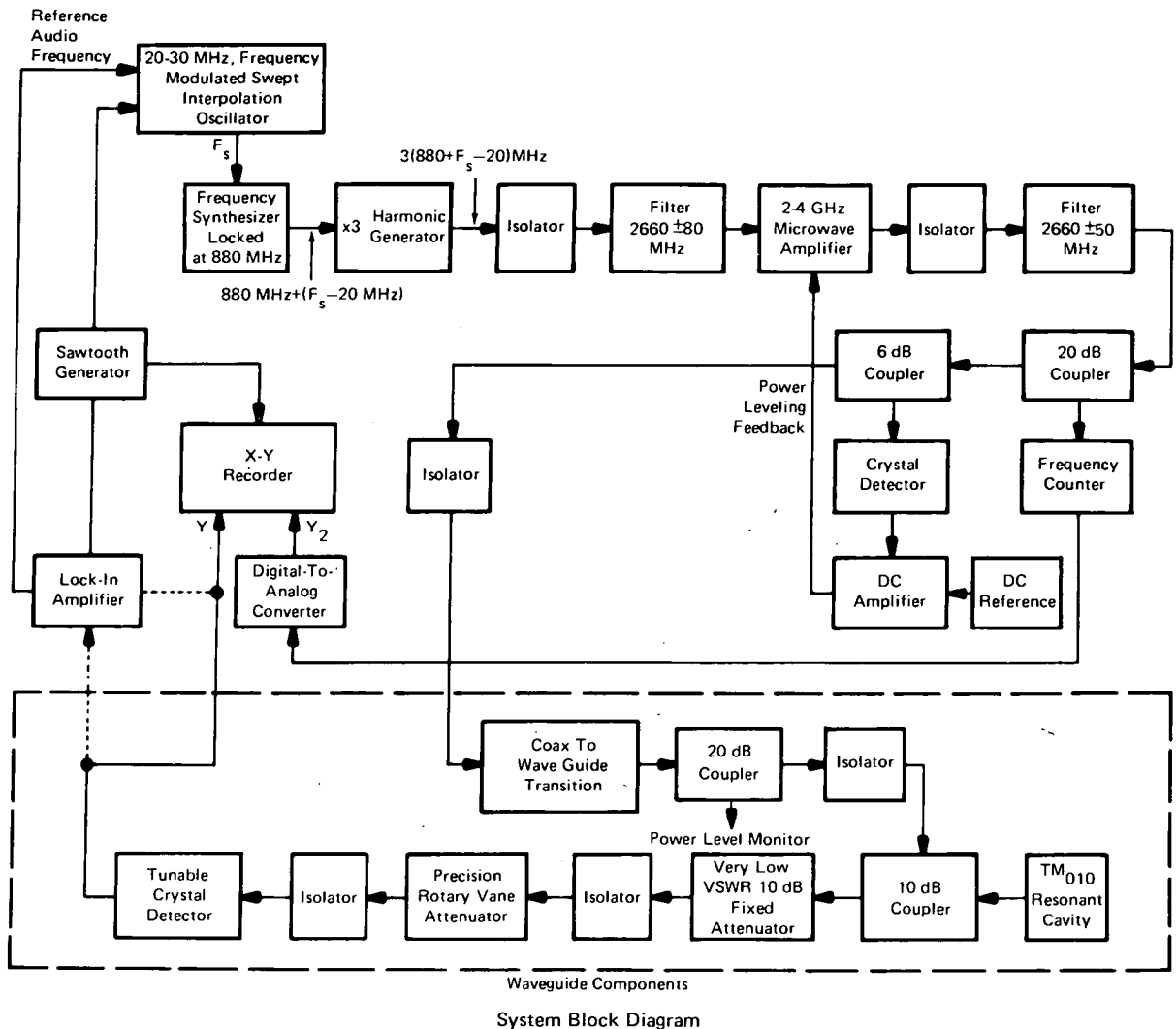
Figure 2. Reed Switch Test Chamber

introduced into the inner chamber, the temperature reduction at the switches was extremely rapid. No pull-in or dropout readings could be obtained during this period.

After temperature stabilization was achieved with liquid helium in the system, readings of pull-in and dropout current for each switch were recorded. The heater coil then was energized, and the switch temperatures were allowed to increase. Curves of pull-in and dropout current as a function of temperature were plotted and were found to be relatively flat.

Circle 11 on Reader Service Card.

IMPROVEMENTS TO MICROWAVE-CAVITY
MEASUREMENTS OF DIELECTRIC CONSTANTS

Reference
Audio
Frequency

20-30 MHz, Frequency Modulated Swept Interpolation Oscillator

F_s

$3(880+F_s-20)$MHz

Frequency Synthesizer Locked at 880 MHz

x3 Harmonic Generator

Isolator

Filter 2660 ±80 MHz

2-4 GHz Microwave Amplifier

Isolator

Filter 2660 ±50 MHz

880 MHz+(F_s−20 MHz)

Sawtooth Generator

Power Leveling Feedback

6 dB Coupler

20 dB Coupler

X-Y Recorder

Isolator

Crystal Detector

Frequency Counter

Y Y_2

Lock-In Amplifier

Digital-To-Analog Converter

DC Amplifier

DC Reference

Coax To Wave Guide Transition

20 dB Coupler

Isolator

Power Level Monitor

Tunable Crystal Detector

Isolator

Precision Rotary Vane Attenuator

Isolator

Very Low VSWR 10 dB Fixed Attenuator

10 dB Coupler

TM_{010} Resonant Cavity

Waveguide Components

System Block Diagram

The shift in the resonant frequency caused by a sample introduced into a microwave cavity is dependent on the dielectric constant of the sample. This technique has been used extensively to measure the dielectric properties of matter. Several recently developed refinements to such standard techniques allow dielectric constants and dielectric loss to be measured with accuracies of 0.1 percent and 0.3 percent, respectively (several times better than existing techniques).

Improvements to conventional methods include the use of a precision microwave cavity and more accurate instrument calibration techniques. In addition, a system has been developed which allows accurate online sensing of samples passing through the cavity.

The apparatus consists of a cylindrical TM_{010} resonant cavity with an axially-symmetric electric field, thus allowing samples to be continuously pumped through the cavity along the field axis. The TM_{010} mode is used because it is not degenerate with other excitable resonances, and cavity dimensions can be designed to eliminate mode mixing.

The figure shows the microwave circuit used to measure the frequency shift and the change of Q in the cavity. Microwave power is generated with a frequency standard accurate to 1 part in 10^7. After multiplication, filtering, and amplification, a power-leveling feedback circuit is used to keep the output power constant as a function of oscillator frequency.

The dc signal at the crystal detector is compared to a dc reference, and the amplified difference voltage is fed back to the microwave amplifier to control the system gain. This keeps residual amplitude modulation below 0.05 percent and long-term drift below 0.02 percent.

The cavity response is measured in the waveguide component. The frequency band measured with this system is accurate to within ±1 kHz, and power levels are accurate to within ±0.05 dB. Accuracy is further improved by FM modulation of the interpolation oscillator with a reference audiofrequency from a lock-in amplifier. With these improvements, frequency measurements may be made to within ±0.2 kHz.

Circle 12 on Reader Service Card.

PLAQUE SURFACE-AREA MEASUREMENT

A method has been developed to accurately measure the electrolyte/electrode interfacial area of nickel plaque used in nickel/cadmium battery cells. Conventional methods, such as the BET gas adsorption technique (Brunnauer, Emmett, and Teller method) and galvanostatic methods, fail to give exact measurements. The BET method yields the area penetrated by the gas (which is not identical to the electrolyte/electrode interfacial area), and galvanostatic measurements are complicated by faradaic currents.

When a solid electrode is immersed in an electrolyte, some charge is adsorbed by the electrode, via the adsorption of ions from the electrolyte. The configuration of charges formed corresponds to a capacitor; the adsorbed layer of ions and a layer of oppositely charged ions in the electrolyte constitute the double-layer capacitance. If the adsorbed charge is represented by q_0 and the capacitance by C, the potential drop between the two layers of charge is V_0, where

$$-V_0 = q_0/C \qquad (1)$$

If the electrode potential is changed by a small amount to V, the charge on the electrode will change to q. With a sudden change in potential, a current flows. When the current returns to zero, a quiescent state is reached so that

$$-V = (q_0+q)/C \qquad (2)$$

Subtracting equation (1) from (2), and solving for C, a useful form is obtained:

$$C = \frac{1}{\eta} \int i(t)dt$$

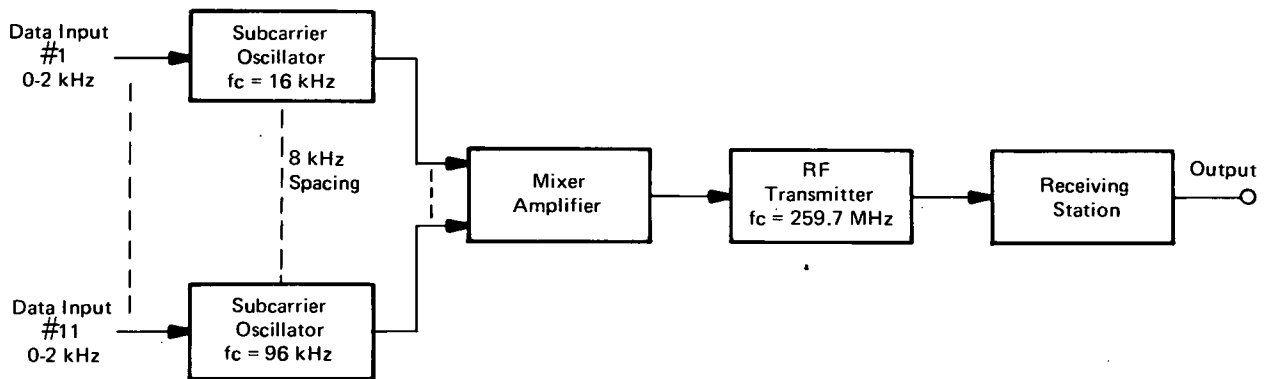where $\eta = V-V_0$. An implicit condition is that $i = 0$ at $t = 0$. Moreover, there is a limit to η. A plot of i_{peak} versus η shows that there is a linear relationship up to 15 mV. Thus, η must not exceed 15 mV.

The potential change is applied to the electrode using a potentiometer, and the current returns to zero within 5 ms. A photograph of an oscillograph trace is made, and q is estimated by integrating the area under the current-time trace. This is used to compute the double-layer capacitance. Then the interface area can be calculated from the standard values of capacitance per unit area for the specific material whose surface area is desired.

No further documentation is available.

END-TO-END RMS ERROR TESTING ON A CONSTANT-BANDWIDTH FM/FM SYSTEM

```
Data Input                    ┌──────────────┐
   #1          ───────────▶   │  Subcarrier  │
 0-2 kHz                      │  Oscillator  │
            ┊                 │  fc = 16 kHz │
            ┊                 └──────────────┘        ┌────────────┐      ┌──────────────┐      ┌────────────┐   Output
            ┊              ┊ 8 kHz                    │            │      │     RF       │      │            │      O
            ┊              ┊ Spacing                  │   Mixer    │ ───▶ │ Transmitter  │ ───▶ │  Receiving │
            ┊              ┊                          │ Amplifier  │      │ fc = 259.7 MHz│      │   Station  │
            ┊              ┊                          └────────────┘      └──────────────┘      └────────────┘
            ┊                 ┌──────────────┐
Data Input  ┊                 │  Subcarrier  │
  #11       ───────────▶      │  Oscillator  │
 0-2 kHz                      │  fc = 96 kHz │
                              └──────────────┘
```

Constant-Bandwidth FM/FM System

The root-mean-square (RMS) testing technique for constant-bandwidth, frequency-modulated communication systems consists of multiple time-dependent sampling, digitalization, differentiation, and division, to determine system error. In this technique, groups of well-established signal-analysis procedures may be combined for use in specific applications. Eleven channels are used as shown in the figure.

The combined effects of intermodulation, adjacent-channel crosstalk, and residual system noise can be determined, as well as the single-channel distortion of the system.

Source: G. R. Wallace
Marshall Space Flight Center and
W. E. Salter of
Sperry Rand Corp.
under contract to
Marshall Space Flight Center
(MFS-22134)

Circle 13 on Reader Service Card.

LOCATION OF WIRING DISCONTINUITIES USING TIME-DOMAIN REFLECTOMETRY

A commercially-available time-domain reflectometer, which was designed to determine the magnitude and nature of discontinuities in high-frequency coaxial cable transmission systems, can also locate and identify discontinuities in standard wiring. A test procedure has been defined to minimize errors and to aid in interpreting results.

Reflections from an impedance mismatch are observed on the oscilloscope. The displacement between the start of the step voltage and the reflection indicates the location of the discontinuity, and the characteristics of the reflection indicate the nature and value of the mismatch.

Source: D. C. King of
Grumman Aerospace Corp.
under contract to
Johnson Space Center
(MSC-12479)

Circle 14 on Reader Service Card.

LIMITATIONS OF CORROSION DETECTION-AND-EVALUATION
EQUIPMENT: A REPORT

A study of the nondestructive evaluation methods and techniques for determining the extent of corrosion on a structure points out the possible drawbacks and the promising aspects of each method and makes improvement suggestions. Methods and techniques discussed are the result of research and experience at NASA, major aerospace companies, equipment suppliers, and universities. The report may be of interest to metal societies, plastic societies, structural firms, and corrosion protection firms.

Six types of corrosion are reviewed: general, galvanic, filiform, pitting, intergranular, and stress. Among the techniques studied are the following: direct and remote viewing; radiography; penetrant; eddy current; pH analysis; chemical spot tests, polarized light reflection; and ultrasonic techniques, including compression wave, delta principle, shear wave, and surface wave.

Source: F. E. Sugg, F. H. Stuckenberg,
and C. C. Kammerer of
Rockwell International Corp.
under contract to
Marshall Space Flight Center
(MFS-24436)

Circle 15 on Reader Service Card.

ASSESSMENT OF NONDESTRUCTIVE TESTING: A REPORT

A technical report presents an assessment of the present capabilities and limitations of nondestructive testing (NDT) as applied to aerospace structures during the design, development, production, and operational phases. The assessment considers two material systems: (1) metal alloy systems and (2) bonded composites, such as honeycomb structures and fiber-reinforced composites. The NDT techniques discussed include radiography, ultrasonics, penetrants, and thermal, acoustic, and electromagnetic methods.

Quantitative and qualitative data are presented in tabular form. No single source exists where the same information has been quantitatively treated. Reliability and standardization methods are presented, and corroborative data with fracture mechanics are given.
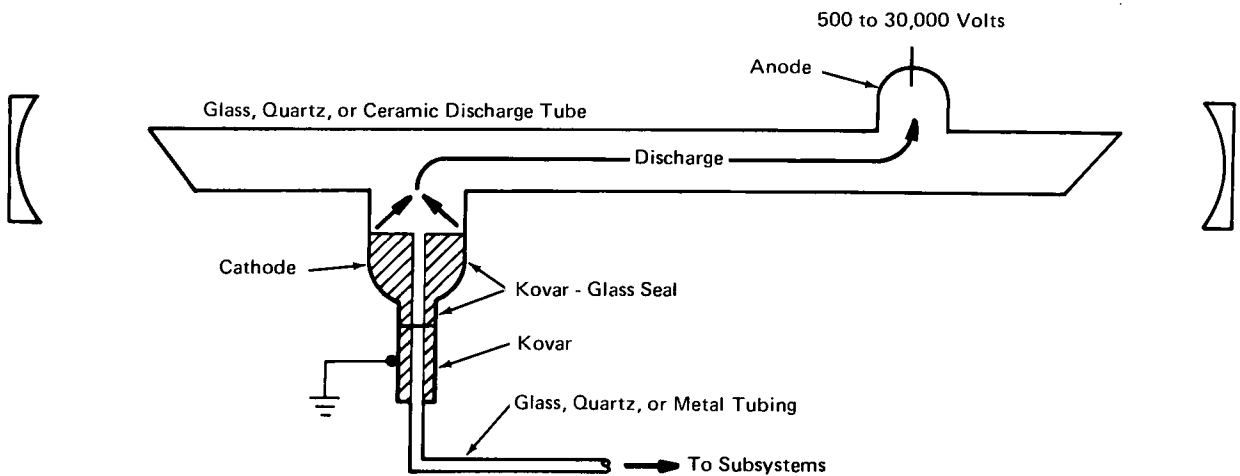
Source: R. W. Neuschaefer and
J. B. Beal of
Marshall Space Flight Center
(MFS-22595)

Circle 16 on Reader Service Card.

Section 3. Analysis of Gases and Gas-Suspensions

TECHNIQUE FOR ELECTRICALLY ISOLATING GAS-LASER SUBSYSTEMS

Schematic of Electrically-Isolated Gas-Laser Discharge Tube

The presence of high electrode voltages (500 to 30,000 volts) in gas-ion lasers makes it necessary to electrically isolate the discharge tube from the rest of the laser system. Isolation prevents the electric discharge from coursing through the laser subsystem rather than through the main discharge tube.

The figure shows the discharge tube-subsystems interface in a typical laser system. A new technique for electrically isolating the subsystems consists of grounding the specially constructed cathode, as shown. The subsystems then are shielded by the grounded cathode and may be grounded themselves without concern for possible discharge from the anode terminating on them. The open center section of the cold cathode in no way reduces the effectiveness of the cathode since emission is confined to small regions around the periphery.

Arrangements for hot-cathode systems and for systems that require the use of a gas-return line are also available. The isolation technique described is applicable to all pulsed-ion laser systems.

Source: C. E. Wood and R. S. Witte of
TRW, Inc.
under contract to
Marshall Space Flight Center
(MFS-22597)

Circle 17 on Reader Service Card.

DETECTION OF NITRIC OXIDE POLLUTION
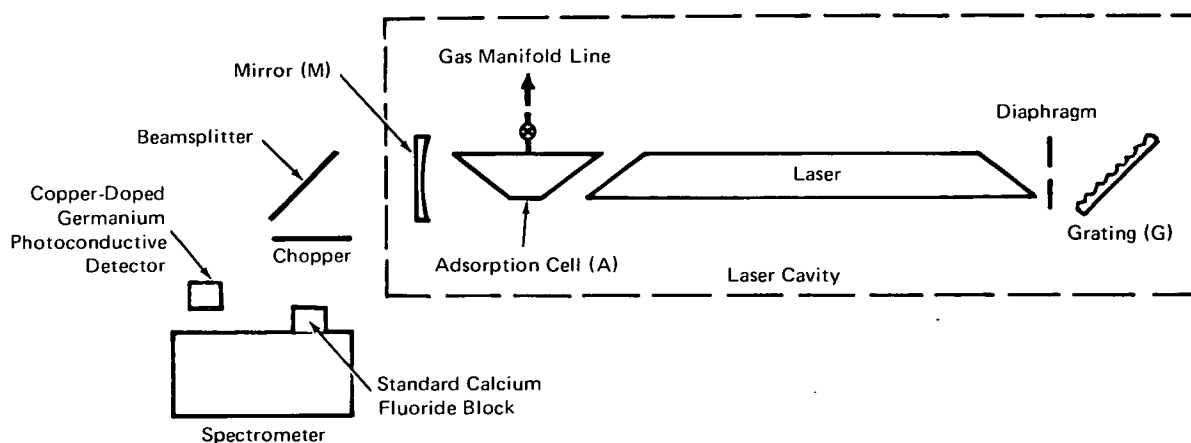
Laser/Spectrophotometer System

Nitric oxide is a major air pollutant and is the precursor to nitrogen dioxide, the trigger molecule in photochemical processes which yield smog. Eye irritation and other discomforts are severe when high levels of nitric oxide are present in the atmosphere. Although new and improved methods are constantly being sought to measure the high levels of nitric oxide in emissions from automobiles and electrical power plant stacks, special techniques are required to measure the low concentrations ordinarily present in the ambient atmosphere.

Studies of the enhancement of absorption spectra of certain atomic and molecular species inserted in dye-laser cavities have indicated that nitric oxide can be determined at low concentrations. For example, at 1900.04 cm^{-1}, the absorption coefficient of small amounts of nitric oxide in an intra-laser-cavity absorption cell containing helium is enhanced by more than two orders of magnitude.

The apparatus used to make absorption measurements is shown in the diagram; the laser cavity is defined by the grating, G, blazed for 5.4 μm, and the 10-percent-transmission mirror M (10-meter radius). The laser has an interelectrode separation of 119 cm, of which 115 cm are immersed in a liquid nitrogen bath. The laser is run in the CW mode, nominally at 10 kV and 15 mA, and the laser as well as the absorption cell, A, are fitted with calcium fluoride Brewster windows. About 10 percent of the laser output is directed through a chopper onto a sanded flat of calcium fluoride placed at the entrance of an infrared

spectrophotometer. The signal is detected by nitrogen-cooled copper-doped germanium, and it is amplified, demodulated by a lock-in amplifier, and displayed on a strip chart. The sensitivity of the laser spoiling to intercavity nitric oxide is enhanced by running the laser at the lowest gain possible.

Mixtures of helium and nitric oxide at pressures of the order of 50 kN/m^2 (0.5 atm) are let into the absorption cell from a gas-handling manifold (not shown in the diagram). For an experimental run, laser power loss measurements are made on successive NO-He mixtures of increasing dilution prepared by expanding a small part of the preceding sample and diluting with helium to about 50 kN/m^2 pressure.

It is anticipated that at nitrogen pressures of about 100 kN/m^2, the sensitivity of the laser output to nitric oxide should be further enhanced because of greater pressure broadening of the NO lines; in view of experimental results, it is estimated that NO concentrations of the order of 100 parts per billion can be easily determined with an intercavity length of 50 cm. Moreover, theoretical considerations suggest that the method is capable of infinite sensitivity, but additional experiments must be performed to establish practical limits.

Circle 18 on Reader Service Card.

LOW-TEMPERATURE AEROSOL-SAMPLING TECHNIQUE
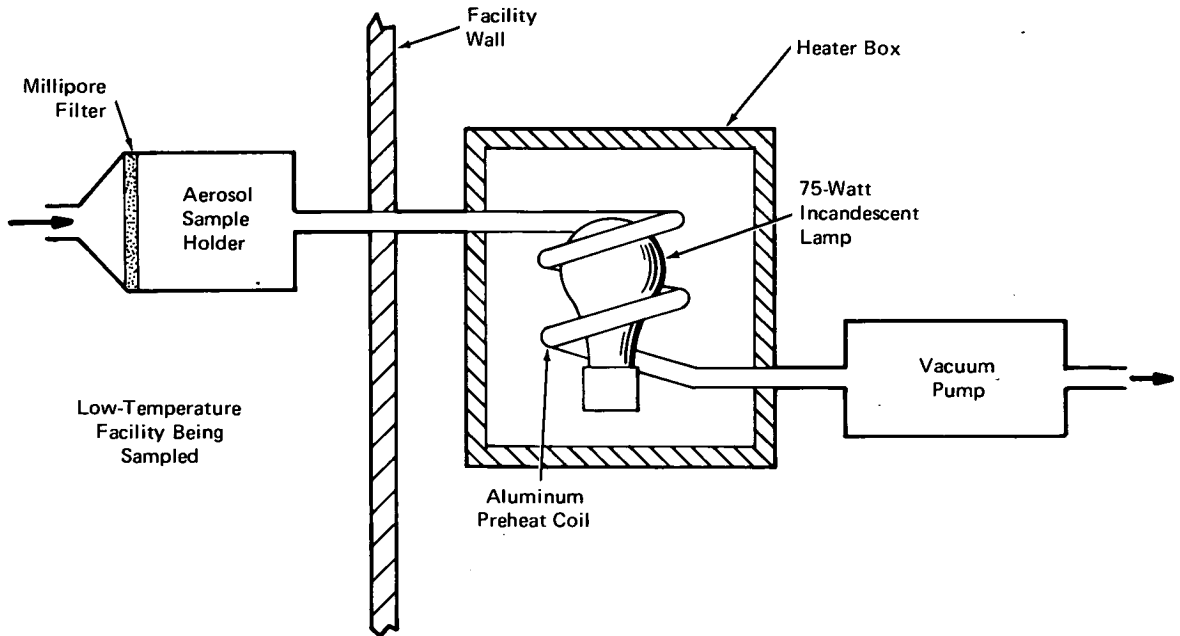
Aerosol sampling is a very reliable method for determining the level of airborne contamination in clean rooms. Such sampling is usually required at least once every 24 hours to determine if cleanliness is being maintained. This procedure is accomplished by the use of a vacuum pump and a particle filter system. Samples are obtained by passing a known flow of air across a membrane filter for a specific period of time. Since the vacuum pump slows down in environments which are colder than room temperature, due to congealing lube oil, it is not possible to obtain the desired flow rate in a low-temperature clean facility [a class A clean-room test facility that operates over a temperature range of 20° to 60° C (68° to 140° F)].

A new technique overcomes this difficulty by locating the vacuum pump outside of the test facility and connecting it to the particle analysis filter inside the chamber by tubing routed through a port in the chamber wall (see figure). A heater box was fabricated to preheat the air coming from the chamber. This heater box consists of a 75-watt incandescent lamp surrounded by an aluminum coil through which the incoming air passes and is preheated to approximately room temperature by the light bulb. An additional advantage of this system results from the consequent decrease in the number of people inside the facility: the average humidity level is minimized.

No further documentation is available.

DETECTION AND MEASUREMENT OF TRACE GASES BY
CORRELATION INTERFEROMETRY: A REPORT

A report, now available, discusses the feasibility of detecting gases in a closed environment by correlation interferometry. The methods discussed are applicable to systems such as those used for detecting toxic, explosive, or polluting gases. Various techniques are available for evaluating gas concentrations, including mass spectroscopy, gas chromatography, and absorption spectroscopy techniques, such as dispersive correlation spectroscopy and nondispersive gas analyzers.

The basic requirements which must be satisfied by a technique if it is to be considered for real-time monitoring are: (a) the capability of completing a gas analysis with only a short (less than 1 minute) delay; (b) the possibility of analyzing many selectable gases during a cycle, with good discrimination between gases (the rejection of interfering gases in the measurement of the target gas); and (c) the possibility of being developed into compact field instrumentation. Correlation interferometry is an analytical technique with the capability of satisfying all of these requirements. The report includes a detailed preliminary investigation of the theoretical maximum sensitivities to certain gases (mainly in the IR region). A theoretical and practical description of the technique is presented, and the results of laboratory tests with specific gases are given.

Seventeen gases were selected for investigation: CH_2O, $COCl_2$, $(CN)_2$, HF, H_2S, NH_3, CO, HCN, CH_4, CH_3Cl, HCl, SO_2, COF_2, $CHCl_3$, NO, NO_2, and 2-Butanone. Except for NO_2 and 2-Butanone, bands suitable for measurement of the gases were found in the 2- to 11-μm region.

In most cases it is possible, on the basis of low-resolution spectra, to find a band for which unattenuated interference from background gases is less than 10 times the toxicity threshold limit value (TLV), or 100 ppm in the absence of an established TLV. With the exception of HCl, an interference level of 1 TLV

(or 10 ppm) should be achievable by providing an interference attenuation factor of less than 10 for most cases and 60 for the worst case.

The signal-to-noise ratios estimated on the basis of laboratory experiments are considerably poorer than expected, due to a high random noise level. However, even for the worst case (CH_4), the signal/noise ratios should be of the order of 1 for a 20-m gas path, estimated on the basis of low-resolution spectra. Reduction of the random noise level in the laboratory instrument should be possible and will improve considerably the signal-to-noise ratios and interferent attenuation factors. Adequate sensitivity should be achievable for almost all gases of interest with an interferometer operating in the region of 2 to 11 μm.

The design of an instrument to handle the measurement of one gas, or the simultaneous measurement of a limited number of gases in the same spectral region, should be straightforward: A self-contained electronics and signal-processing system would probably be adequate. If the number of gases to be handled is large, the incorporation of a minicomputer for signal processing (as was done in the laboratory) might be preferable. Measurements of all gases could be made every few seconds, if not limited by output display device speeds. With low random noise levels, small sample paths would be adequate. Otherwise multiple-path sample volumes may be used.

Circle 19 on Reader Service Card.

DYNAMIC TECHNIQUE FOR MEASURING ADSORPTION IN A GAS CHROMATOGRAPH

Chromatograph Peak
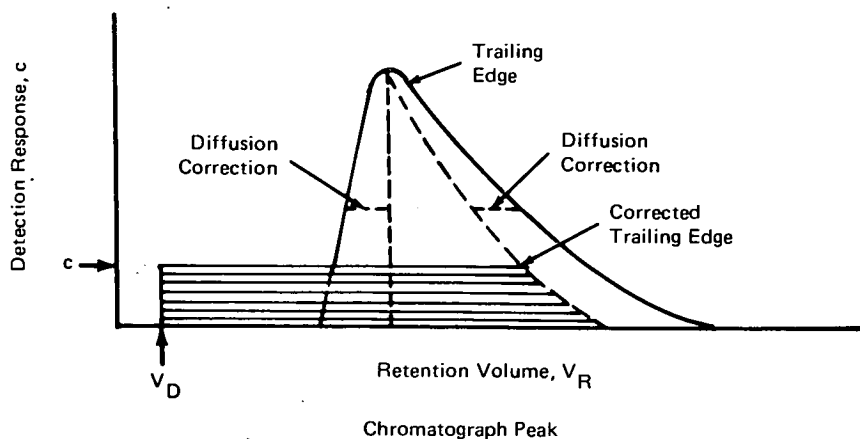
The adsorption characteristics of a compound can be obtained with the help of a gas chromatograph. However, when studying the adsorption of materials at low concentrations (less than 1 ppm) the standard technique requires several hours.

A dynamic gas-chromatographic procedure, together with a mathematical analysis of the adsorption isotherm, allows relative surface areas and adsorptive powers for trace concentrations to be determined in a few minutes.

The adsorbent (charcoal for instance) heated in vacuum until it is free of all adsorbed compounds, is packed in a gas-chromatograph column. The retention volume of the compound of interest is measured in a temperature-controllable chromatograph. An inert gas such as nitrogen is used as a carrier.

The solid curve in the figure outlines a typical peak observed on the chromatograph. The shape of the trailing edge can be corrected for diffusion, by assuming that the front edge deviates from a vertical line due to diffusion alone. The dotted curve shows the corrected edge, assuming diffusion broadened the trailing edge by the same amount that it broadened the leading edge. The detector response can be calibrated in terms of concentration by setting the total area under the curve equal to the amount of adsorbate used.

It can be shown that the time required for a point on the tail of the peak to pass through the column is proportional to the slope of the isotherm, at the point corresponding to the concentration in the tail, and that the adsorption isotherm can be found by integrating the tail of the chromatographic peak according to

$$f(c) = \int_0^c f'(c)\, dc = \int_0^c \frac{V_R - V_D}{m}\, dc$$

where:

V_R (c) is the retention volume for the tail of a chromatographic peak corresponding to a gas-phase concentration of "c";

m is the mass of the solid phase;

f (c) is the adsorption isotherm evaluated at "c" with f' (c) as the first derivative; and

V_D is the dead space.

In the figure, then, the shaded area represents

$$mf(c) = \int_0^c V_R - V_D\, dc$$

and can be evaluated for all values of c from 0 to the peak height.

This technique may be used to evaluate the relative surface areas of different adsorbates, expressed as a volume of adsorbent/gram of adsorbate, and to evaluate their relative adsorptive power.
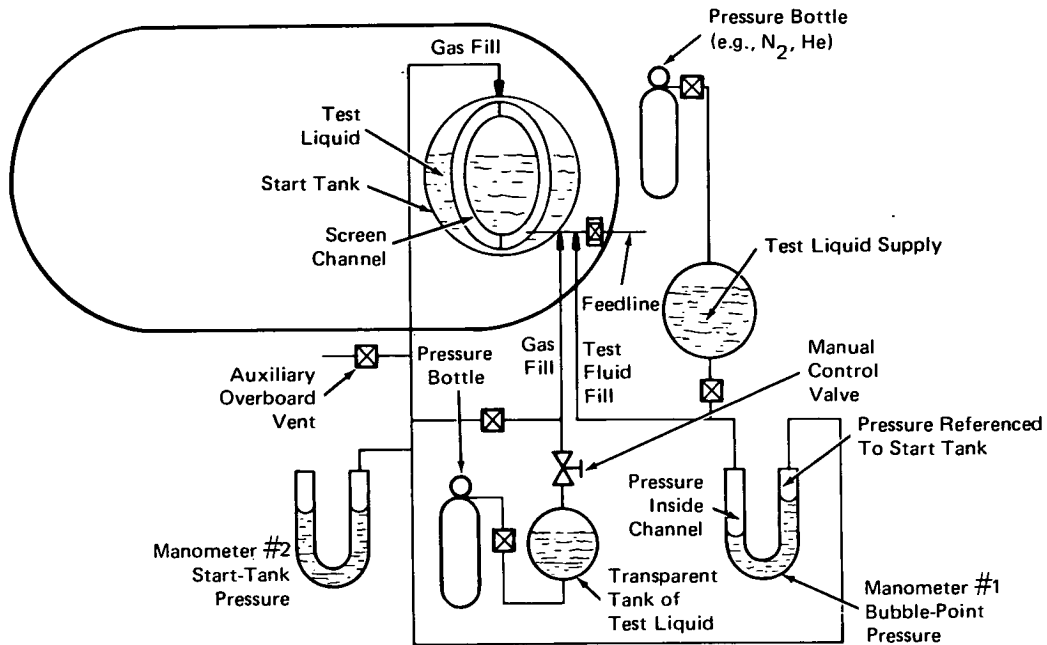
The following documentation may be obtained from:

National Technical Information Service
Springfield, Virginia 22151
Single document price $3.00
(or microfiche $2.25)

Reference: NASA CR-115202 (N71-37657), A Study of Physiochemical Factors Affecting Charcoal Adsorption of Contaminants in Manned Spacecraft Atmosphere

LARGE-SCALE BUBBLE-POINT TEST TECHNIQUE

Bubble-Point Verification Procedure

A technique has been developed for verifying the average pore dimensions of mesh screen used in the construction of large devices. A major advantage of the system is that, unlike conventional bubble-point test systems, it is not necessary to immerse an entire screen in the test liquid. The figure shows the basic setup, as used to verify the pore size of a screen channel in a cryogenic propellant system.

The pore size is related to the pressure at which a liquid film on the screen will break. In this test the screen, a tubular channel, is wetted; and a pressure differential is created between the inside of the screen and the surrounding start tank. The seal of liquid film on the channel screen is verified by bubbling a gas through a transparent vessel into the channel. If bubbles leave the liquid and migrate into the channel, the seal is not complete.

There are several ways of wetting the screen; a total-immersion system is shown in the figure. The tank is filled with the test liquid which wets the screen. Then the liquid is purged by a gas fed into the start tank, both inside and outside the channel to keep pressures identical on both sides of the screen. Pressures inside and outside of the screen are measured by two separate manometers.

Two other methods have been developed to wet the screen without total immersion. These are particularly useful when the screen device is large. In the first method the screen is wetted by spraying it with the test liquid; the second method is by condensation. Laboratory tests were made to prove that if a saturated vapor is introduced at a temperature slightly higher than that in the tank, condensation will form a film over the pores of the screen.

This system is an improvement over previous methods in that: (a) Large screens in tanks can be tested without removing them; (b) The bubble point can be verified for screen devices larger than the supportable height of a liquid column; and (c) The problem of transient heat transfer is alleviated during the bubble-point test, since the test-fluid condensation brings the entire tank to a steady-state temperature equal to that of the surroundings.

Circle 20 on Reader Service Card.

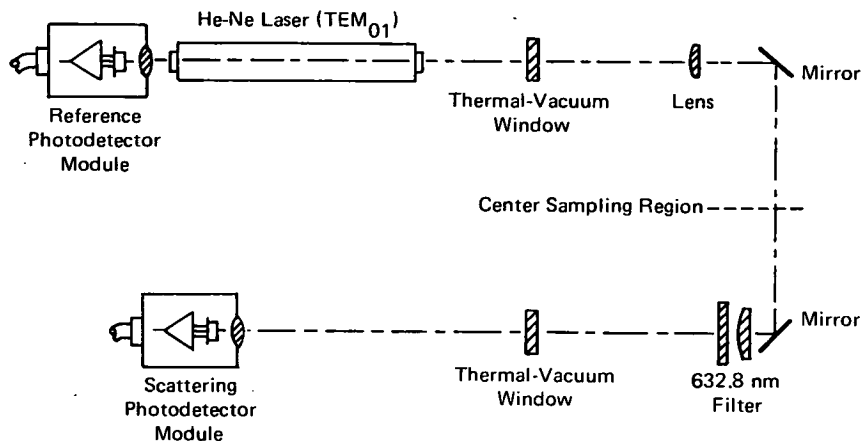# PARTICLE ANALYSIS BY ACTIVE SCATTERING-PARTICLE SPECTROMETRY

Figure 1. Optical System, Forward-Scattering Spectrometer
(Particle Size Range: 0.2 to 0.6 μm)

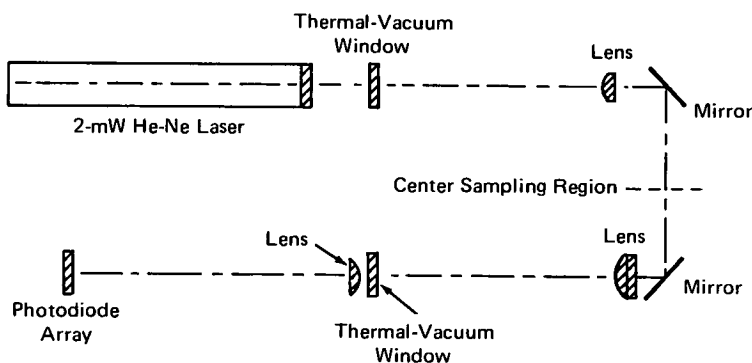Figure 2. Optical System, Optical Array Spectrometer
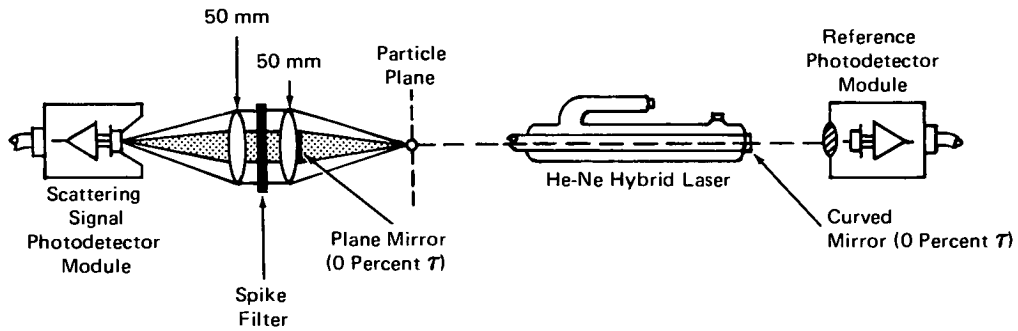(Particle Size Range: 4 to 32 μm)

Three spectrometry systems have been developed to determine the sizes and velocities of particles in the air. The spectrometers could be used for the environmental monitoring of particulate pollution, for clean-room monitoring experiments, or for other particle-counting jobs where real-time data on small particles is needed.

Figure 1 shows a forward-scattering spectrometer that detects particles ranging from 0.2 to 0.6 micrometers in size. Particles passing through the beam in the sampling region scatter light out of the collimated beam; and the

photodetector measures this scattered light, the intensity of which is proportional to particle size.

The spectrometer in Figure 2 images the shadows of particles passing through the sample area on the photodiode array. Particle size can be calculated by determining how many diodes are within a shadow. These two systems employ simple digital logic circuits to process the data and read them out as realtime histograms.

Figure 3. Optical System, Active-Scattering Particle Spectrometer
(Particle Size Range: 0.1 to 1.5 μm)

In the third system two circuits are used as indicated in Figure 3. One unit covers a range of particle sizes from 0.1 to 1.5 micrometers, and the second unit covers a range from 1 to 25 micrometers.

Source: J. R. Williams and
D. M. Russell of
Marshall Space Flight Center
(MFS-22621)

Circle 21 on Reader Service Card.

ELECTROSTATIC PARTICULATE-QUANTITY MEASUREMENT SYSTEM

Millivoltmeter

Sensing Element

Air Intake

Teflon or
Nylon

Vacuum Pump
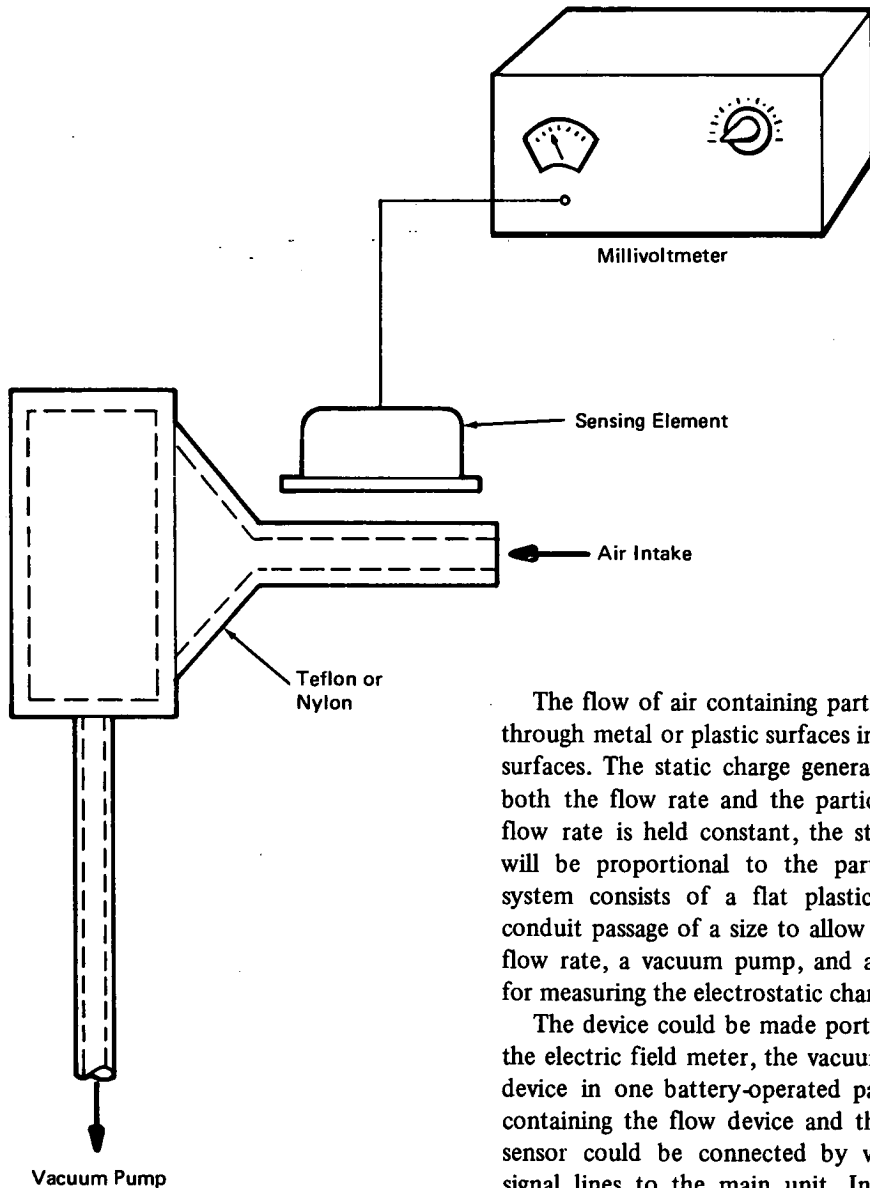
The flow of air containing particulate matter over or through metal or plastic surfaces induces a charge on the surfaces. The static charge generated is proportional to both the flow rate and the particulate content. If the flow rate is held constant, the static charge generated will be proportional to the particulate content. The system consists of a flat plastic flow device with a conduit passage of a size to allow for a sufficiently-high flow rate, a vacuum pump, and an electric field meter for measuring the electrostatic charge.

The device could be made portable by encompassing the electric field meter, the vacuum pump, and the flow device in one battery-operated package. Also, a probe containing the flow device and the electric field meter sensor could be connected by vacuum and electrical signal lines to the main unit. In addition, a recorder could be connected for continuous monitoring.

The system indicated in the figure provides a sensitive method of measuring particulate quantity in the air. This enables an index to be established for comparing particulate contamination levels of industrial atmospheres.

Source: J. B. Johnston
Marshall Space Flight Center
(MFS-22128)

Circle 22 on Reader Service Card.

Patent Information

The following innovations, described in this Compilation have been patented or are being considered for patent as indicated below:

**Real Time Statistical Analysis of Acoustic Emission Signals
for Flaw-Monitoring Systems (Page 9) MFS-24402**

Inquiries concerning rights for the commercial use of this invention should be addressed to:

> Patent Counsel
> Marshall Space Flight Center
> Code CC01
> Marshall Space Flight Center, Alabama 35812

Plaque Surface-Area Measurement (Page 19) LAR-11427

Inquiries concerning rights for the commercial use of this invention should be addressed to:

> Patent Counsel
> Langley Research Center
> Code 313
> Hampton, Virginia 23665

Technique for Electrically Insulating Gas-Laser Subsystems (Page 22) MFS-22597

Title to this invention has been waived under the provisions of the National Aeronautics and Space Act [42 U.S.C. 2457(f)], to TRW, Inc., Redondo Beach, California 90278.

Electrostatic Particulate-Quantity Measurement System (Page 30) MFS-22128

This invention is owned by NASA, and a patent application has been filed. Inquiries concerning nonexclusive or exclusive license for its commercial development should be addressed to:

> Patent Counsel
> Marshall Space Flight Center
> Code CC01
> Marshall Space Flight Center, Alabama 35812

Notes: